Lateral interactions among phospholipid head groups at the heptane/water interface

ARTICLE *in* LANGMUIR · JANUARY 1988

Impact Factor: 4.46 · DOI: 10.1021/la00079a037

2 AUTHORS, INCLUDING:

Ken A Dill
Stony Brook University
389 PUBLICATIONS **27,712** CITATIONS

SEE PROFILE

acid probably takes place at the triple bonds provided by the first exposure.

Conclusions

For the photoresist in the semiconductor photolithography, the study was extended to the five LB films for EX laser, i.e., TDA, PDA, HDA, OAA, and ω-TCA. Especially, fabrication of resist pattern with the KrF EX stepper and spectroscopic evaluation were carried out.

(1) In terms of the pattern shape and photosensitivity, PDA for EX laser gave the best result. With PDA films, a 0.3-μm pattern could be fabricated by the EX stepper.

(2) The photoreactivity with the molecular arrangement of LB films was investigated in detail. It was demonstrated that the photoreactivity of PDA LB films for KrF EX laser was influenced strongly by the molecular arrangement.

Future studies will include the impermeability to plasma under various conditions, and, for the purpose of a detailed study of photoreaction processes of PDA LB films, IR or Raman spectroscopic analysis will be carried out.

This technique should become useful for the fabrication of 64-Mbit D-RAMs, if higher efficiency can be achieved in the preparation of LB films.

Acknowledgment. We thank Dr. H. Mizuno of Matsushita Electric Ind. Co., Ltd., Semiconductor Research Center and Prof. T. Takenaka of the Kyoto University Chemical Research Laboratory for their kind advice.

Registry No. $CH_3(CH_2)_9$—C≡C—C≡C—$(CH_2)_8$—COOH, 66990-30-5; $CH_3(CH_2)_{11}$—C≡C—C≡C—$(CH_2)_8$—COOH, 66990-32-7; $CH_3(CH_2)_{13}$—C≡C—C≡C—$(CH_2)_8$—COOH, 67071-94-7; HC≡C—$(CH_2)_{20}$—COOH, 111625-23-1; $CH_3(CH_2)_{17}$—CH=CHCOOH, 111625-22-0.

Lateral Interactions among Phospholipid Head Groups at the Heptane/Water Interface

Dirk Stigter and Ken A. Dill*

Departments of Pharmaceutical Chemistry and Pharmacy, University of California, San Francisco, California 94143

Received June 4, 1987. In Final Form: August 11, 1987

The strong lateral repulsions among phosphatidylcholine head groups in monolayers and bilayers, and their large positive dependence on temperature, have long been considered puzzling. Here we analyze the careful and extensive experiments of Taylor et al. on the lateral pressure–area isotherms of phosphatidylcholine molecules at low density at the heptane/water interface to determine the second and third virial coefficients. We investigate the possible origins of these repulsions through consideration of the in-plane and out-of-plane dipole interactions among the zwitterions and among the carbonyl groups. We show that spectroscopic and thermodynamic experiments are consistent only with a model in which the principal dipolar repulsion arises from a small average out-of-plane displacement of the N^+ end of the head group, surprisingly directed back toward the oil phase, rather than into the water phase, and increasing with temperature. The repulsion between head groups is enhanced significantly by out-of-plane dipole fluctuations.

1. Introduction

Phospholipids are fundamental constituents of biological membranes. Their interactions dictate to a large extent the structures and properties of bilayers and membranes. The most direct way to study the interactions and to determine the equation of state among phospholipids is through measurement of lateral pressure–area isotherms at an oil/water interface. Extensive experiments are available on dialkylphosphatidylcholine (PC) monolayers at the heptane/water interface.[1-3] It is observed that at low surface densities the lateral pressure is independent of the ionic strength of the aqueous phase (10^{-3}–10^{-1} M NaCl) and of the lengths of the hydrocarbon tails of the phospholipids (studied in the range C_{14} to C_{22}). Therefore, at these low densities the origin of nonideal lateral mixing must be principally interactions among the uncharged head groups. The experiments show that these PC head group interactions are repulsive and that the repulsion increases with temperature.[2] Models presented heretofore have not been able to account for these observations. The authors of the experimental studies concluded[3] that: "No satisfactory explanation of the high repulsion is available and its large positive temperature coefficient runs counter to the expected behaviour of dipole and water-structuring forces."

Our purpose is to develop molecular theory to account for these interactions. The work presented in this paper is comprised of two parts. (i) We analyze the low density pressure–area isotherms of Taylor et al.[2] in terms of the two-dimensional virial expansion, and we express deviations from ideal behavior in terms of B_2 and B_3, the second and third virial coefficients. (ii) On the basis of NMR spectroscopic data, and X-ray and neutron scattering evidence reviewed by several authors,[4-6] we consider molecular models of the various head group interactions from which we predict the virial coefficients.

We develop and test several simple models for the steric and dipolar contributions to the lateral interactions among zwitterionic head groups. In section 4 below, we express

(1) Yue, B. Y.; Jackson, G. M.; Taylor, J. A. G.; Mingins, J.; Pethica, B. A. *J. Chem. Soc., Faraday Trans. 1* **1976**, *72*, 2685.
(2) Taylor, J. A. G.; Mingins, J.; Pethica, B. A. *J. Chem. Soc., Faraday Trans. 1* **1976**, *72*, 2694.
(3) Mingins, J.; Taylor, J. A. G.; Pethica, B. A.; Jackson, G. M.; Yue, B. Y. T. *J. Chem. Soc., Faraday Trans. 1* **1982**, *78*, 323.
(4) Seelig, J.; Seelig, A. *Q. Rev. Biophys.* **1980**, *13*, 19.
(5) Büldt, G.; Wohlgemuth, R. *J. Membr. Biol.* **1981**, *58*, 81.
(6) Davis, J. H. *Biochim. Biophys. Acta* **1983**, *737*, 117.

0743-7463/88/2404-0200$01.50/0

Table I. Exponents in Equations 1 and 2 Derived from Lateral Pressure–Area Isotherms of Dioctadecylphosphatidylcholine Monolayers Spread between *n*-Heptane and 0.01 M NaCl in Ref 2

T, °C	c_2	c_4
5	2.508	2.505
10	2.350	2.266
15	2.240	2.264
20	2.212	2.205
25	2.078	2.131

the electrostatic free energy of dipolar interaction in terms of the relative coordinates of the dipole charges of the two interacting head groups. The various dipolar models are based on this interaction potential. In section 5, we consider an array of dipoles uniformly distributed over a plane and oriented normal to the interface, and we show that the concentration dependence of Π disagrees with that of the experiments. Thus, in section 6, we consider a two-dimensional virial expansion instead. We consider two models for the steric contribution to the head group repulsion: hard disks and hard elongated shapes. We show this steric contribution to B_2 to be approximately 100 Å^2, and not much different for the two models, so we subsequently consider hard disks a suitable approximation for the steric repulsion. We then consider the contribution from dipoles uniformly displaced normal to the interface, but laterally with a Boltzmann pair distribution, in evaluations of B_2. This model is shown to give a good description of the experimental data. Thus we then describe other details relevant to this model. In section 7, we show that the in-plane component of the dipole interaction is attractive, but very small. In section 8, we show that dipole fluctuations normal to the interface are important, and in section 9, we briefly consider the third virial coefficient.

2. Representation of Pressure–Area Experiments

We consider the pressure–area isotherms of dioctadecylphosphatidylcholine monolayers spread at the interface between *n*-heptane and 0.01 M NaCl, reported by Taylor, Mingins, and Pethica[2] at 5-deg intervals from 5 to 25 °C. We have extracted the data from an enlarged copy of Figure 1 of ref 2. We consider representation of these data in two different forms: in terms of an approximate expression (eq 1), derived from a lattice van der Waals approach[7] that treats all surface densities, and in terms of a lowest order virial expansion (eq 2):

$$\frac{\Pi}{kT} = \frac{1}{A_0} \ln \frac{A}{A - A_0} + c_1\left(\frac{1}{A}\right)^{c_2} \quad (1)$$

$$\frac{\Pi}{kT} = \frac{1}{A} + c_3\left(\frac{1}{A}\right)^{c_4} \quad (2)$$

where Π is the lateral pressure, k is Boltzmann's constant, T is the absolute temperature, A is the area per lipid molecule, and A_0 = 40.0 Å^2 is the hard core minimum area per lipid molecule in compressed monolayers used in ref 7. c_2 = 2 in the lattice theory and c_4 = 2 in the truncated virial expansion, but all the c's are just taken here to be parameters to test the utility of eq 1 and 2 for representing the data. The best fit for the isotherms in Figure 1 of ref 2 was determined from plots of log $[\Pi/kT - (1/A_0) \ln \{A/(A - A_0)\}]$ and of log $(\Pi/kT - 1/A)$ versus log $(1/A)$. The slopes, c_2 and c_4, of the best straight lines on such plots are given in Table I. These results show that, when the data are fit to eq 1 and 2, the exponents c_2 and c_4 are found to be nearly equal and definitely larger than 2. This is evidence that neither of these expressions adequately describes the data. Therefore, inasmuch as the virial expansion is exact, we consider below addition of the higher order terms in the virial expansion.

(7) Cantor, R. S.; Dill, K. A. *Langmuir* **1986**, *2*, 331.

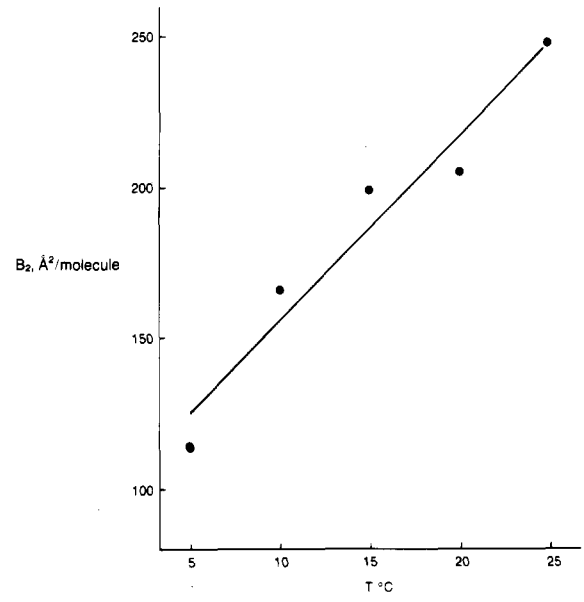

Figure 1. Second virial coefficient B_2 of dioctadecylphosphatidylcholine at the heptane/water interface from 5 to 25 °C. Points lateral pressure–area isotherms by Taylor, Mingins, and Pethica.[2] Solid line, least-squares linear fit.

The two-dimensional virial expansion of the lateral pressure is

$$\frac{\Pi}{kT} = \Gamma + B_2\Gamma^2 + B_3\Gamma^3 + \ldots \quad (3)$$

where $\Gamma = 1/A$ is the surface concentration of the lipid. The second and third virial coefficients are evaluated from a least-squares fit of the experimental values of $\Pi/kT - \Gamma$ to the two-term polynomial $B_2\Gamma^2 + B_3\Gamma^3$. Each experimental isotherm yields a B_2 value, which is shown as a point in Figure 1. The line in Figure 1 is the least-squares linear fit as a function of temperature.

The B_3 values obtained above show a large scatter as a function of temperature. This scatter is reduced as follows. The straight line in Figure 1 gives smoothed B_2 values that are now used to calculate, from each experimental isotherm, values of $\Pi/kT - \Gamma - B_2\Gamma^2$, which are then (least-squares) fitted to $B_3\Gamma^3$. This has the advantage of using all the data to give reliable estimates of B_2 and B_3 at a given temperature. The following discussion is based on the smoothed values of B_2 and the values of B_3 obtained with them in this fashion.

The experimental isotherms are compared with the virial expansions in Figures 2 and 3, which show $\Pi/kT\Gamma^2 - 1/\Gamma$ versus Γ as points, while the lines represent $B_2 + B_3\Gamma$. The use of two figures here simply serves to prevent overlapping of data points. The deviation of the points from the relevant lines corresponds, on average, to 0.042 dyn/cm in Π, compared with a reported experimental error of 0.05 dyn/cm.[1] The error bars around the 5 °C line in Figure 2 are for $\Delta\Pi = \pm 0.04$ dyn/cm. The considerable scatter of the points in Figures 2 and 3 shows that the present experiments do not give significant information on the virial coefficients beyond B_3. Therefore, in the concentration range under study, the nonideality of the monolayers will be described as interactions between pairs and triplets of head groups.

The values of B_2, B_3, and of the ratio B_3/B_2^2 for the various temperatures are collected in Table II. The trends

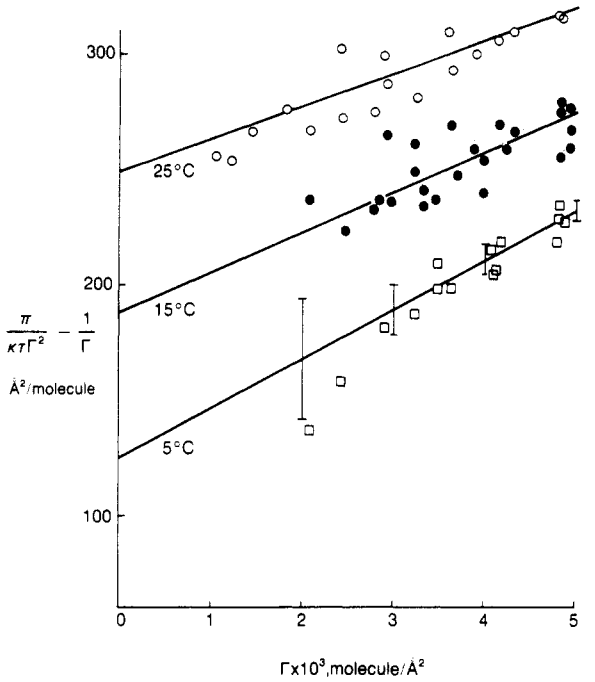

Figure 2. Plots of $\Pi/kT\Gamma^2 - 1/\Gamma$ ($= B_2 + B_3\Gamma + ...$) versus Γ of dioctadecylphosphatidylcholine at the heptane/water interface at 5, 15, and 25 °C for the determination of B_2 and B_3. Points from Π versus $1/\Gamma$ data by Taylor, Mingins, and Pethica.[2] Straight lines and error bars, see text.

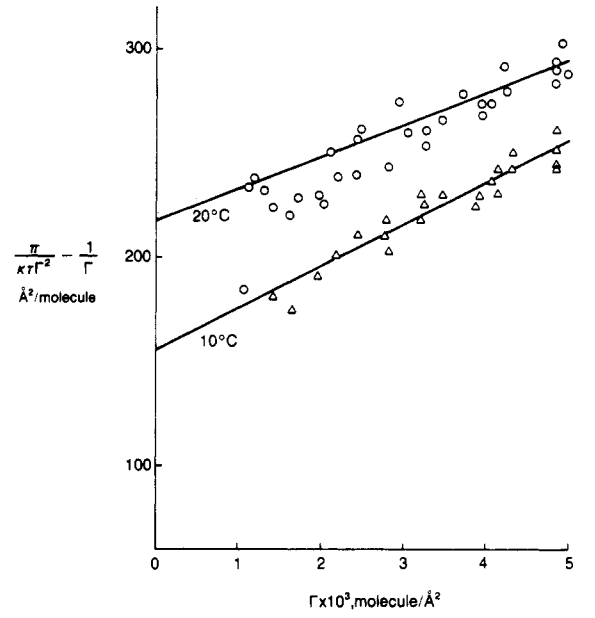

Figure 3. Plots of $\Pi/kT\Gamma^2 - 1/\Gamma$ ($= B_2 + B_3\Gamma + ...$) versus Γ of dioctadecylphosphatidylcholine at the heptane/water interface at 10 and 20 °C for the determination of B_2 and B_3. Points from Π versus $1/\Gamma$ data by Taylor, Mingins, and Pethica.[2] Straight lines, see text.

with temperature are very pronounced. At 5 °C the result for B_2, 125 Å²/molecule, is not much higher than the value expected for a hard disk model of the head group (see below). The large increase of B_2 with temperature, to 249 Å²/molecule at 25 °C, is strong evidence of increasing repulsion between the head groups. For hard disks with area A_0 we have[8] $B_2 = 2A_0$ and $B_3/B_2^2 = 0.782$. In general one expects B_2, and also the ratio B_3/B_2^2, to depend on the shape of the head group and on their interactions.

(8) Ree, F. H.; Hoover, W. G. *J. Chem. Phys.* **1967**, *46*, 4181.

Table II. Two-Dimensional Second and Third Virial Coefficients Derived from Experimental Lateral Pressure–Area Isotherms of Dioctadecylphosphatidylcholine Monolayers Spread between *n*-Heptane and 0.01 M NaCl in Ref 2

T, °C	B_2, Å²/molecule	B_3, Å⁴/molecule	B_3/B_2^2
5	125	21.7×10^3	1.39
10	156	20.1×10^3	0.826
15	187	17.8×10^3	0.511
20	218	15.4×10^3	0.324
25	249	14.7×10^3	0.237

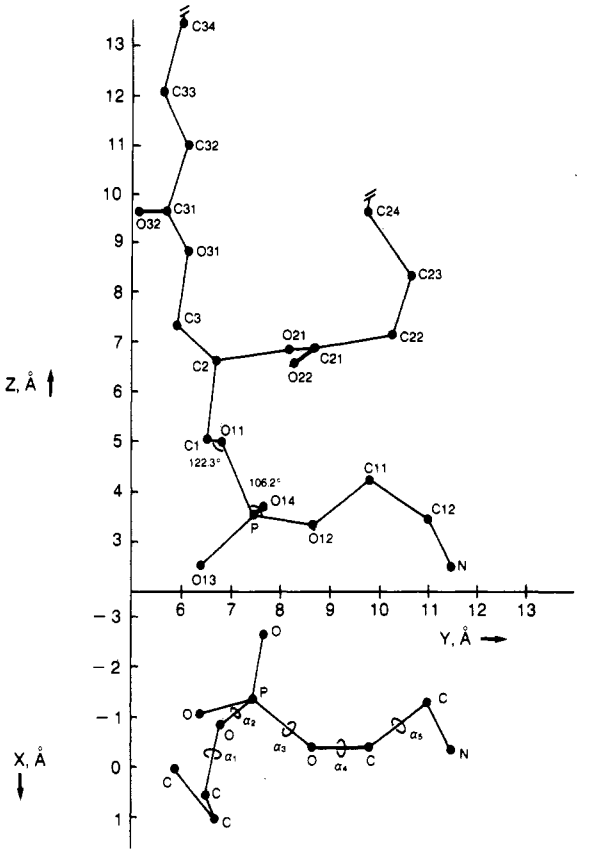

Figure 4. Partial projection of phosphatidylethanolamine (PE) head group on *xy* (bilayer plane) and *yz* planes from X-ray structure of 1,2-dilauroylphosphatidylethanolamine–acetic acid[9] with notation of Sundaralingam.[10] In the *zy* projection the hydrocarbon tails are omitted beyond C24 and C34, in the *xy* projection beyond C2 and C3.

3. Head Group Conformation

As a basis for an interaction model of the PC head group on monolayers, we discuss its conformation in bilayers, for which experimental data are more readily available. The phosphatidylethanolamine (PE) head group is included in the discussion because it has many features in common with PC.

The principal conclusion from structural methods is that the P–N dipole of the head group lies approximately parallel to the bilayer plane. Hitchcock et al.[9] report the X-ray analysis of 1,2-dilauroylphosphatidylethanolamine–acetic acid. The single crystals have the classical lipid bilayer structure. Partial projections of a single molecule on the *xy* and *zy* planes are shown in Figure 4, with the notation of Sundaralingam.[10] The bond angles in the phosphoryl group are those from the X-ray study

(9) Hitchcock, P. B.; Mason, R.; Thomas, K. M.; Shipley, G. G. *Proc. Natl. Acad. Sci. U.S.A.* **1974**, *71*, 3036.
(10) Sundaralingam, M. *Ann. N.Y. Acad. Sci.* **1972**, *195*, 324.

of L-α-glycerolphosphorylethanolamine monohydrate by DeTitta and Craven.[11] Different conformations are produced by changing one or more of the torsion angles α_i. Hauser et al.[12] list eight different sets of α_i values, as determined crystallographically for various PC and PE constituents. Typical in all cases is the arrangement of the P–N chain roughly parallel with the xy bilayer plane, with the C1–C2–C3 glycerol backbone approximately perpendicular to it. Worchester and Franks[13] and Büldt et al.[14] have confirmed this general arrangement directly in PC bilayers and model membranes by neutron diffraction.

Much information, albeit more indirect, has been obtained also by other spectroscopic techniques, in particular by ^2H NMR of selectively deuteriated compounds and by ^{31}P NMR.[4-6] The data exclude complete rigidity of the head group, as well as complete rotational freedom around all bonds, but are consistent with a fairly rigid glycerol backbone, restricted rotation in the P–C12 link, and free rotation around the N–C bonds. A model in agreement with the NMR data, studied by Seelig, Gally, and Wohlgemuth,[15] is a PC head group with rapid transitions between two enantiotropic forms determined in single crystals.[12] The model shows that the calculated NMR data are quite sensitive to a variation in torsion angles: a decrease of α_5 by 1° caused the same change of the $C12D_2$ NMR signal as lowering the temperature by approximately 20 °C. It is interesting that such a decrease of α_5 moves the $N(CH_3)_3$ group toward the aqueous phase, which, as shown below, would weaken dipolar repulsions between head groups and, therefore, lower B_2. So the trend with temperature of the NMR data is consistent with the trend of B_2 in Table II, in both cases indicating the same direction of movement of the N^+ end of the head group dipole, toward water when the temperature decreases.

Unfortunately, the available NMR information has been insufficient for a unique determination of the torsion angles. Skarjune and Oldfield[16] have shown that many conformations are consistent with the NMR data. In addition, without further information, the average conformational contributions and the motional effects, involving fluctuations which are rapid on the NMR time scale, cannot be separated in the NMR data.

Neutron diffraction, on the other hand, yields information not only on the average position, but also on the positional fluctuations of the scattering deuterons. Büldt et al.[14] report results on PC model membranes with selectively deuteriated methylene groups. For the root mean square fluctuation along the bilayer normal, μ, they report in the gel phase at 20 °C $\mu = 0.9 \pm 0.4$ Å for the C2D and $\mu = 2.1 \pm 0.5$ Å for the $C12D_2$ fragment and in the liquid crystalline phase at 70 °C $\mu = 2.6 \pm 0.5$ Å for $C12D_2$. In general, the μ values measure fluctuations in the position of the two deuterons in methylene groups and include out-of-layer fluctuations of the entire molecule, as well as long-range imperfections of the membranes in the crystal lattice. In $C12D_2$ μ includes also head group fluctuations which, however, cannot be separated from the rest without knowing the orientatin of the $C12D_2$ fragment. The results for $C12D_2$ are, therefore, a measure of the maximum value of μ of C12.

In PC and PE liquid crystalline phases with up to 50 mol % cholesterol, Brown and Seelig[17] have found that the changes in $C12D_2$ NMR signals are comparable with those caused by an increase of temperature in cholesterol-free bilayers.[18] This indicates that cholesterol, serving as a spacer between the lipid molecules, causes only small changes in the head group conformation. It is reasonable to expect that above the melting temperature conformations of the head groups will be relatively insensitive to changes of density, and therefore that they will be similar in bilayers and in monolayers at an oil/water interface.

On the basis of the evidence summarized above, we assume that in PC and PE monolayers the head groups are approximately coplanar with the oil/water interface, while the glycerol backbone is perpendicular to it. The glycerol group with its ester linkages is fairly rigid; restricted rotation, mainly through α_4 and α_5, and free rotation around the N–C bonds give the remainder of the head group a considerable flexibility, which increases toward the distal nitrogen.

Inasmuch as the evidence shows that the moment of the PN dipole lies largely in-plane, and inasmuch as free dipoles in two dimensions should attract rather than repel (see below), several workers[19,20] have assumed that the principal out-of-plane moment must derive from the ester moieties C21 and C31. We find no compelling evidence for this point of view however. The total dipole moment of most esters in the gas or liquid phase is about 1.8 D/molecule,[21] compared with about 20 D for the P^-–N^+ zwitterion of PC and PE head groups. In the structure depicted in Figure 4 the C21 ester group and the C31 carbonyl are nearly parallel with the layer plane. Accepting this as representative for orientations in monolayers, the total ester contribution to the normal component of the dipole moment is probably less than 1 D. In contrast, the relatively strong dependence on temperature of the interaction between head groups requires a normal dipole moment up to several debyes per head group; this is shown below. For these reasons we concentrate on the contribution of the zwitterion.

Dipole interactions are consistent with the observed insensitivity to ionic strength of the PC head group repulsions.[2] Formally, one might assume a Debye–Hückel ionic atmosphere of small ions near each of the head group charges. However, inasmuch as the distance between the head group charges is much shorter than the Debye length, the two ionic atmospheres largely overlap and, hence, neutralize each other. Thus, the dipole field around a head group is essentially unmodified by the salt, and head group interactions are insensitive to ionic strength, as observed experimentally.

4. Interactions between Dipoles

We consider two dipoles representing two different head groups, each located at the sharp interfacial boundary between water, with dielectric constant ϵ_w, and n-heptane, with dielectric constant ϵ_h. Although interfacial fluctuations occur, the effective interface region is expected to be thin compared with the lateral distances of head group

(11) DeTitta, G. T.; Craven, B. M. *Acta. Crystallogr., Sect. B: Struct. Crystallogr. Cryst. Chem.* **1973**, *B29*, 1354.
(12) Hauser, H.; Pascher, I.; Pearson, R. H.; Sundell, S. *Biochim. Biophys. Acta.* **1981**, *650*, 21.
(13) Worchester, D. L.; Franks, N. P. *J. Mol. Biol.* **1976**, *100*, 359.
(14) Büldt, G.; Gally, H. U.; Seelig, J.; Zaccai, G. *J. Mol. Biol.* **1979**, *134*, 673.
(15) Seelig, J.; Gally, H. U.; Wohlgemuth, R. *Biochim. Biophys. Acta* **1977**, *467*, 109.
(16) Skarjune, R.; Oldfield, E. *Biochemistry* **1979**, *18*, 5903.
(17) Brown, M. F.; Seelig, J. *Biochemistry* **1978**, *17*, 381.
(18) Gally, H. U.; Niederberger, W.; Seelig, J. *Biochemistry* **1975**, *14*, 3647.
(19) Flewelling, R. F.; Hubbell, W. L. *Biophys. J.* **1986**, *49*, 541.
(20) Raudino, A.; Mauzerall, D. *Biophys. J.* **1986**, *50*, 441.
(21) Smyth, C. P. *Dielectric Behavior and Structure*, McGraw-Hill: New York, 1955.

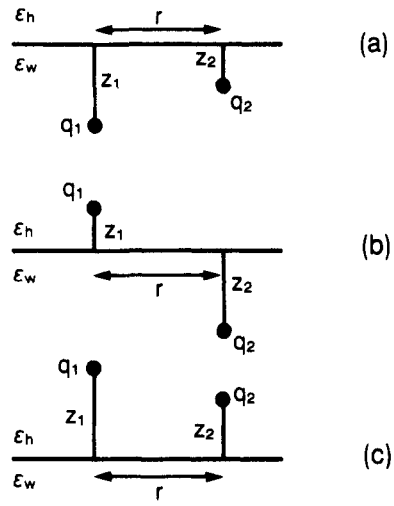

Figure 5. Point charges near the heptane/water interface, with interactions given by eq 4–6.

interactions, so a step function of the dielectric constant, from ϵ_w to ϵ_h, is a good approximation. The dipole interactions between the head groups are calculated by summing the Coulombic contributions between the single dipolar charges, which are obtained as follows. Let the respective distances of charges q_1 and q_2 from the interface be z_1 and z_2, and let r be the projection of the distance between the charges on the interface, as shown in Figure 5. It is well-known that the dielectric boundary conditions may be satisfied with the method of image charges,[22] leading to the following results for the interaction potential U between q_1 and q_2:

$$U = \frac{q_1 q_2}{4\pi\epsilon_0\epsilon_w}\left[\frac{1}{(r^2 + (z_1 - z_2)^2)^{1/2}} + \frac{\epsilon_w - \epsilon_h}{(\epsilon_w + \epsilon_h)(r^2 + (z_1 + z_2)^2)^{1/2}}\right] \quad (4)$$

for q_1 and q_2 in water, Figure 5a, where ϵ_0 is the permittivity of vacuum

$$U = \frac{q_1 q_2}{2\pi\epsilon_0(\epsilon_w + \epsilon_h)(r^2 + (z_1 + z_2)^2)^{1/2}} \quad (5)$$

for q_1 in water and q_2 in heptane or vice versa, Figure 5b

$$U = \frac{q_1 q_2}{4\pi\epsilon_0\epsilon_h}\left[\frac{1}{(r^2 + (z_1 - z_2)^2)^{1/2}} - \frac{\epsilon_w - \epsilon_h}{(\epsilon_w + \epsilon_h)(r^2 + (z_1 + z_2)^2)^{1/2}}\right] \quad (6)$$

for q_1 and q_2 in heptane, Figure 5c.

Equations 4–6 are symmetrical with respect to the interacting charges and their coordinates, as expected.

Figure 6 shows three different arrangements with respect to the interface of the z-axis projection of two dipoles, both with moment de, with a distance r between them. For one of the dipoles in heptane, Figure 6a, the set of image charges across the interface is also shown.

Electrostatic interaction energies are additive. So the total interaction between two different groups of charges i and j near an interface, such as the dipoles in Figure 6, is obtained by applying to each pair of charges ij the appropriate equation, eq 4, 5 or 6, and summing the results. For two dipoles in oil, Figure 6a, we obtain

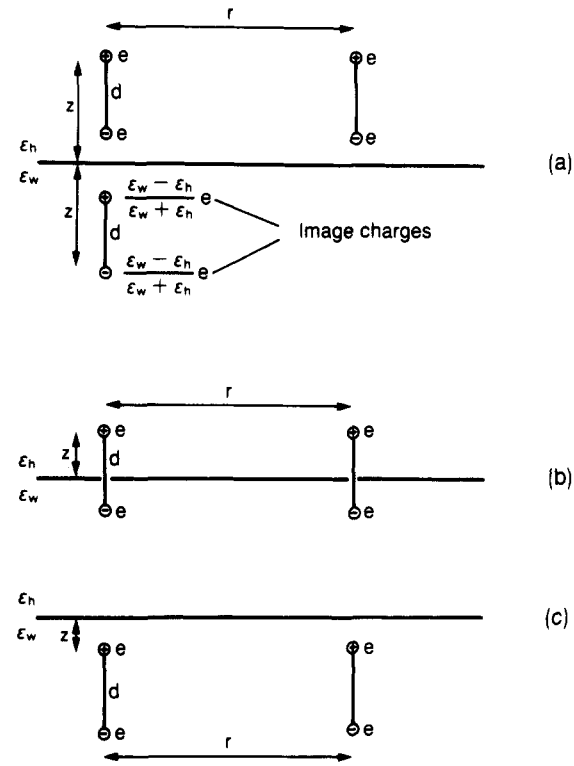

Figure 6. Dipole charges near the heptane/water interface, with interactions described in eq 8–12.

$$U = \frac{e^2}{4\pi\epsilon_0\epsilon_h}\left[\frac{2}{r} - \frac{2}{(r^2 + d^2)^{1/2}} + \frac{\epsilon_w - \epsilon_h}{\epsilon_w + \epsilon_h}\left\{\frac{2}{(r^2 + (2z - d)^2)^{1/2}} - \frac{1}{(r^2 + 4z^2)^{1/2}} - \frac{1}{(r^2 + (2z - 2d)^2)^{1/2}}\right\}\right] \quad (7)$$

Expansion of the expression in square brackets in eq 7 for $r \gg z + d$ yields

$$\frac{d^2}{r^3}\frac{2\epsilon_w}{\epsilon_w + \epsilon_h} + O\left(\frac{1}{r^5}\right) \quad (8)$$

So for large distance r between the dipoles in heptane, Figure 6a, the limit of eq 7 may be written as

$$U = \epsilon_w{}^2 f \qquad f \gg z + d \quad (9)$$

where

$$f = \frac{e^2 d^2}{4\pi\epsilon_0 r^3}\frac{2}{\epsilon_w\epsilon_h(\epsilon_w + \epsilon_h)} \quad (10)$$

With the dipoles in water, Figure 6c, a similar derivation gives, again in terms of eq 10 for f,

$$U = \epsilon_h{}^2 f \qquad r \gg z + d \quad (11)$$

For dipoles which straddle the heptane/water interface, as in Figure 6b, U is between the above cases:

$$U = \left[\frac{z}{d}\epsilon_w + \left(1 - \frac{z}{d}\right)\epsilon_h\right]^2 f \qquad r \gg d \quad (12)$$

Since $\epsilon_w \gg \epsilon_h$, we may use $U = \epsilon_w{}^2 f z^2/d^2$ as an approximation to eq 12. It is clear from eq 9 and 10 that this is equivalent to having one charge at the interface and the other charge at a distance z into the heptane. Comparing this approximation to the unapproximated situation of one

(22) Smythe, W. R. *Static and Dynamic Electricity*; McGraw-Hill: New York, 1968.

charge at a depth z in the heptane and the other at a distance $d - z$ into the water, we have found differences in interaction calculations (of B_2 below) to be insignificant. This illustrates an interesting aspect of the effect of the dielectric boundary on dipole interactions, namely, that in Figure 6b the dipole interaction depends strongly on the distance z of the one (positive) charge into the heptane but the interaction is insensitive to the distance $d - z$ of the other (negative) charge into the water.

The above equations will be used for the interaction between average out-of-plane dipole components given by the coordinate z. Allowing for fluctuations, we shall also deal with dipoles with different out-of-plane components, specified by z_1 and z_2. In this case the pairwise interaction can again be written as a sum of Coulomb interactions, now in terms of z_1 and z_2, which for $z_1 = z_2 = z$ reduces to one of the cases above of average dipole interaction.

5. Uniform Dipole Distribution

It is difficult to give a complete interaction treatment for an accurate model with the geometry and the internal degrees of freedom of the PC head group. Given the above potentials for pairwise interaction, our approach is to investigate several simple models of the contributions of the head group interactions to the lateral pressure–area isotherms. We have recently shown that when head groups are ionic, rather than dipolar, the nonidealities of the pressure–area isotherms at low surface densities can be accounted for by a Gouy–Chapman treatment of a uniformly charged interface, provided it is properly corrected for the discrete ion effect.[23] In the same vein, here we calculate the lateral pressure Π as a function of lipid concentration Γ for a uniform distribution of dipoles. We show that this model does not well predict the dependence of Π on Γ.

We assume parallel dipoles, all of which are perpendicular to the interface. Let the interaction (free) energy between a dipole and all its neighbors, averaged over all possible lateral spatial distributions of the dipoles, be U'. Then the total dipole contribution to Π is

$$\Pi_{el} = \frac{\Gamma}{2} U' \tag{13}$$

The factor 2 is inserted to avoid counting each pair twice.

We assume, on the basis of eq 8–12, that the interaction between two dipoles at distance r from each other decays as C/r^3. We calculate U' for a dipole at the center of a disk with radius r_0, given by $\pi r_0^2 = 1/\Gamma$, surrounded by a dipole sheet with constant density Γ for $r > r_0$ representing the uniformly smeared neighbor dipoles. This interaction is

$$U' = \int_{r_0}^{\infty} \frac{C}{r^3} \Gamma(2\pi r)\, dr \propto \frac{\Gamma}{r_0} \propto \Gamma^{3/2} \tag{14}$$

and with eq 13

$$\Pi_{el} = \text{const}\Gamma^{5/2} \tag{15}$$

This treatment of the dipole sheet may be improved by assuming that the central dipole is distributed uniformly over the area inside $r = r_0$, instead of fixed at the center of the disk. It was found that this more difficult evaluation of U' changes only the constant in eq 15 but not the exponent of Γ.

The factor $\Gamma^{5/2}$ in eq 15 is now compared with results derived from the experimental isotherms. As discussed above, at 5 °C B_2 is relatively small, and the hard-core repulsions between head groups dominate; in this case we find for the exponents in eq 1 and 2 c_2 and $c_4 \cong 2.5$. On the other hand, at 25 °C the large B_2 value in Table II suggests strong dipole repulsions, and we find the exponents c_2 and $c_4 \cong 2.1$ (Table I). The significant disagreement between this low value and the exponent 2.5 in eq 15 is our reason for not pursuing the uniform dipole distribution any further. We now proceed with the virial method.

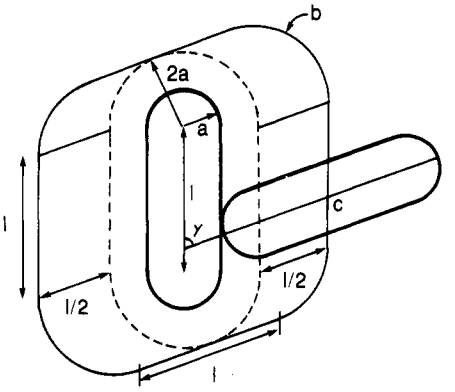

Figure 7. Sketch for derivation of eq 17.

6. Second Virial Coefficient for Disklike Head Groups: Effects of Shape and Dipole Repulsion

Since the smeared dipole approximation above is not a good predictor of lateral pressure, we now consider the more rigorous approach of the two-dimensional virial expansion. The dependence of the two-dimensional second virial coefficient B_2 on the pair potential $U_{12} = U(r_1 r_2)$ is given by[24,25]

$$B_2 = -\frac{1}{2A} \int \int (e^{-U_{12}/kT} - 1)\, dr_1\, dr_2 \tag{16}$$

where r_1 and r_2 are the (sets of) coordinates that define the positions and orientations of particles 1 and 2 in the plane with area A. For hard, circular disks with radius a, when the pair potential is $U_{12} = \infty$ for overlap and $U_{12} = 0$ otherwise, the well-known result is[8] $B_2 = 2\pi a^2$.

We now consider a better approximation to hard-core interaction of the head groups. We assume that the head groups are rectangles of length l, width $2a$, and have semicircular ends with radius a (see Figure 7), and we calculate the second virial coefficient B_2. With a constant angle γ between the particle axes, the mutually excluded area, $2B_2(\gamma)$, is circumscribed by the curve b in Figure 7, which is the path of the center C of the one particle when it moves in contact around the other. Curve b consists of four straight line pieces, each of length l, and four rounded corners which together form a circle of radius $2a$. The surface area enclosed by curve b is

$$2B_2(\gamma) = l^2 \sin\gamma + 8al + 4\pi a^2 \tag{17}$$

Averaging over relative orientations of the particles with

$$B_2 = \frac{1}{\pi} \int_0^{\pi} B_2(\gamma)\, d\gamma \tag{18}$$

eq 17 yields

$$B_2 = \frac{l^2}{\pi} + 4al + 2\pi a^2 \tag{19}$$

(23) Stigter, D.; Dill, K. A. *Langmuir* **1986**, *2*, 791.

(24) Hill, T. L. *J. Phys. Chem.* **1959**, *63*, 456.

(25) Hill, T. L. *Introduction to Statistical Thermodynamics*; Addison-Wesley: Reading, 1960; Chapter 15.

(26) Maitland, G. C.; Rigby, M.; Smith, E. B.; Wakeham, W. A. *Intermolecular Forces*; Clarendon: Oxford, 1981, p 13.

(27) Hill, T. L. *Statistical Mechanics*; McGraw-Hill: New York, 1956; p 203.

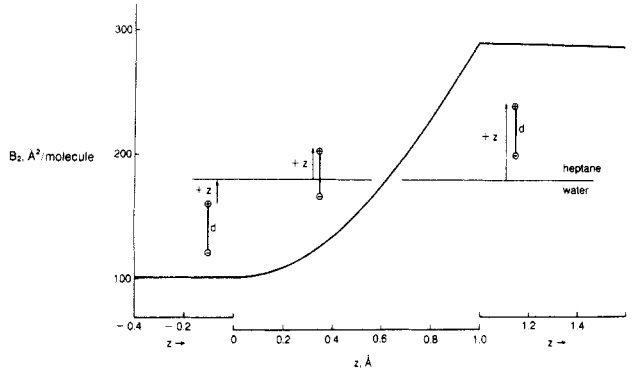

Figure 8. B_2 as a function of position of dipoles with respect to the heptane/water interface, measured by distance z of +e charge into heptane.

In condensed PC monolayers the closest packing area is 45 ± 2 Å²/head group.[1] The PC head groups are somewhat elongated, with an axial ratio of the order of 2. Considering the conformation of PE in Figure 4, van der Waals radii of 1.4 Å for O, 2 Å for CH_3, and 1.5 Å for the NC bond length, we take a 10 × 5 Å model for the PC head group, that is, $l = 2a = 5$ Å in Figure 7. These values give a surface area of 44.6 Å²/head group and, with eq 19, B_2 = 97.2 Å². On the other hand, a circular disk model with the same surface area yields B_2 = 89.2 Å², which is not much smaller than the foregoing result. For head groups with dipole repulsion the influence of shape should be even less. We conclude that the differences in shape contribute insignificantly to the hard-core part of B_2. Therefore our purposes below are satisfied by the simpler approximation that the hard cores are circular disks. In the following we assume a disk model of the PC head group with a radius a = 4 Å, that is, a hard-core B_2 = 100.5 Å².

We now turn to the dipole contributions to B_2. We first consider disks with a constant central dipole perpendicular to the interface, for charge configurations as in Figure 6, with d = 1 Å and with a range of z values. The constant distance between the dipole charges, d = 1 Å, is chosen as the maximum projection of the head group dipole on the normal. We assume that the two head group dipoles are fixed at the same distance normal to the interface, as in Figure 6. Equation 16 becomes

$$B_2 = 2\pi a^2 - \frac{1}{2}\int_{2a}^{\infty}(e^{-U_{12}/kT} - 1)2\pi r\, dr \qquad (20)$$

The integration interval is divided into parts. In the long-range part, from r = 60 Å to $r = \infty$, we have $r \gg z$ and $U_{12} \ll kT$, so $-(e^{-U_{12}/kT} - 1) = U_{12}/kT$ is given by eq 9–12, and the integration is analytic. In the remaining interval, from $r = 2a$ = 8 Å to r = 60 Å, numerical integration is carried out with a pair potential derived from eq 4–6.

Results of this evaluation of eq 20 are shown in Figure 8, where, from left to right, the charges move from water, with ϵ_w = 78.5, into heptane, with ϵ_h = 2. During this transfer B_2 shows three regimes, indicated on the z-axis in Figure 8, which correspond to the three different dipole interaction energies in eq 11, 12, and 9.

When both charges are in water, B_2 is essentially constant and equal to the hard-core value of about 100 Å², because the dipole contribution to B_2 is very small. This agrees with eq 11 where U is proportional to the small quantity ϵ_h^2. On the other hand, when both charges are in heptane, U is much larger, proportional to ϵ_w^2, and B_2 is around 290 Å². In the intermediate region the dipoles are crossing the interface and according to eq 12 U changes with z approximately as $z^2\epsilon_w^2$. This explains the nearly

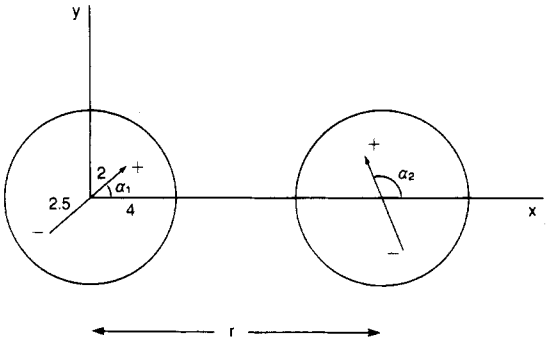

Figure 9. Coordinates for evaluation of B_2 with eq 21.

quadratic increase of B_2 in the central part of the curve in Figure 8.

We now compare the present results with the B_2 values in Table II. The intermediate regime in Figure 8 spans the experimental values, from B_2 = 125 Å² at 5 °C to B_2 = 249 Å² at 25 °C, corresponding to z = 0.33–0.87 Å. This means that if one charge is at the interface, or in the water, the other charge must be 0.33–0.87 Å from the interface into the heptane.

From these results we conclude that one of the head group charges must be displaced into the heptane relative to the other. It is most reasonable to expect that it is the N^+ end of the head group that is displaced into the heptane. The reasons are as follows. The phosphoryl group is the most hydrophilic group on the molecule. Because it is covalently linked to the glycerol backbone and the alkyl chains, which are tightly held in the heptane, the phosphoryl group should be firmly anchored at the interface. The driving forces are far weaker for the trimethylammonium end of the head group. This view is supported by neutron scattering experiments[14] that show that, as mentioned earlier, the root mean square fluctuation of the C2D group near the P^- charge is μ = 0.9 ± 0.5 Å, whereas for the $C12D_2$ fragment near the N^+ charge fluctuations are μ = 2.1 ± 0.5 and 2.6 ± 0.5 Å. The larger fluctuations must correspond to a shallower potential well. Thus we suggest that the P^- of the head group is anchored rather firmly at the interface and that it is the N^+ end which is displaced into the heptane. This displacement increases as temperature increases.[28]

From the considerations of the out-of-plane dipolar repulsive contributions to the lateral pressure, it is clear that dipoles in the water phase interact much too weakly to account for the experimentally observed values of B_2. However, because in crossing the interface the pair potential changes inversely with the square of the dielectric constant, the dipolar repulsion in the oil phase is 3 orders of magnitude larger than the dipolar repulsion in the water phase. Thus less than a 1-Å displacement of the N^+ end of the P^-–N^+ dipole into the oil phase satisfactorily accounts for the large repulsion reflected in the experimentally observed B_2.

7. Effects of Tangential Dipole Component on Second Virial Coefficient

The preceding calculations consider only the out-of-plane component of the dipole moment. Here we consider effects of the in-plane component, which may be attractive or repulsive, depending on the angular orientation of the head groups. One expects that, on the average, the first-order effects cancel due to symmetry, as they do for freely

(28) Dill, K. A.; Stigter, D. submitted for publication in *Biochemistry*.

Table III. Charges and Coordinates for Calculation of U_{12} in Equation 21 for Interaction Model in Figure 9

i	charge	q_i	x_i	y_i	z_i
1	N^+	e	2.0 cos α_1	2.0 sin α_1	z
2	N^+ image	$-e(\epsilon_w - \epsilon_h)/(\epsilon_w + \epsilon_h)$	2.0 cos α_1	2.0 sin α_1	$-z$
3	$P^- + P^-$ image	$-2e\epsilon_h/(\epsilon_w + \epsilon_h)$	2.5 cos $(\alpha_1+\pi)$	2.5 sin $(\alpha_1+\pi)$	0

j	charge	q_j	x_j	y_j	z_j
1	N^+	e	r + 2.0 cos α_2	2.0 sin α_2	z
2	P^-	-e	r + 2.5 cos$(\alpha_2+\pi)$	2.5 sin $(\alpha_2+\pi)$	0

orienting dipoles in three-dimensional bulk solution.[26]

Our computations are based on the model in Figure 9, where the xy plane is the interface. The head groups are hard, circular disks with radius a = 4 Å. The P^- charge is 2.5 Å from the center, at the interface, and the N^+ charge on the opposite side of the disk is 2 Å from the center and a distance z from the interface into the heptane. The relative angular orientation of the disks is given by the angles α_1 and α_2, measured from the vector of length r between the two centers.

A length of the P^-N^+ vector of 4.5 Å in the model is realistic. However, the disk model is an oversimplification inasmuch as it permits separations down to 1.5 and 2.0 Å between the PO_2^- and $N^+(CH_3)_3$ groups of one disk, respectively, with an adjacent disk. These values are less than the van der Waals radii. Therefore, the model of Figure 9 yields an upper limit for the effects on B_2 of the asymmetry of the charge distribution in PC head groups.

In terms of the relative coordinates r, α_1, and α_2, eq 16 for B_2 becomes

$$B_2 = 2\pi a^2 - \frac{1}{4\pi}\int_{r=2a}^{\infty}\int_{\alpha_1=-\pi}^{\pi}\int_{\alpha_2=-\pi}^{\pi}(e^{-U_{12}/kT} - 1)r\,dr\,d\alpha_1\,d\alpha_2 \quad (21)$$

Using eq 4–6 for $r > 2a$, we evaluate U_{12} as the energy of interaction of one head group, with charges q_j, in the potential field of the other head group with charges q_i. With the relevant charges and coordinates from Table III we have

$$U_{12} = \frac{1}{4\pi\epsilon_0\epsilon_h}\sum_{i=1}^{3}\sum_{j=1}^{2}\frac{q_iq_j}{r_{ij}} \quad (22)$$

$$r_{ij} = ((x_i - x_j)^2 + (y_i - y_j)^2 + (z_i - z_j)^2)^{1/2}$$

The integrations in eq 21 were carried out for z values from 0 to 1 Å. The average angular dependence of U_{12} cancels for long distances $r > b$ = 60 Å. Therefore, in the triple integration in eq 21 the long-range contribution from $r = b$ to $r = \infty$ is the same as in eq 20 and, with eq 9, yields $e^2z^2\epsilon_w/\{2\epsilon_0\epsilon_h kTb(\epsilon_w + \epsilon_h)\}$. For the shorter range interval, from $r = 2a$ = 8 Å to $r = b$ = 60 Å, the triple integration in eq 21 was carried out numerically with eq 22, using the symmetry with respect to $\alpha_1 = 0$ to reduce the integration range from $\alpha_1 = 0$ to π.

In Figure 10 the results are compared with those of eq 20 for the same z values. It appears that eq 21 yields smaller values of B_2, showing that the dipole component parallel to the interface provides a net attraction between the head groups. However, the effects are small, a reduction of B_2 of a maximum of 10 Å^2. Since this calculation gives an upper bound, the result shows that the total in-plane contribution can be neglected.

8. Second Virial Coefficient with Dipole Fluctuations

We now turn to fluctuations of the dipole component perpendicular to the interface. We assume that the P^- charge remains fixed at the interface and that the distance z between the N^+ charge and the interface fluctuates. We have to abandon the two-dimensional model and treat the interactions from a more general point of view. Hill[24] has derived the appropriate virial expansion for a solution bounded by an adsorbing surface. When molecules are in an adsorption field $U(z)$ perpendicular to the adsorbing surface, for example, in a quadratic potential well, their fluctuations in the z direction influence the pair interaction potential U_{12}, which is to be used in eq 20 for B_2.

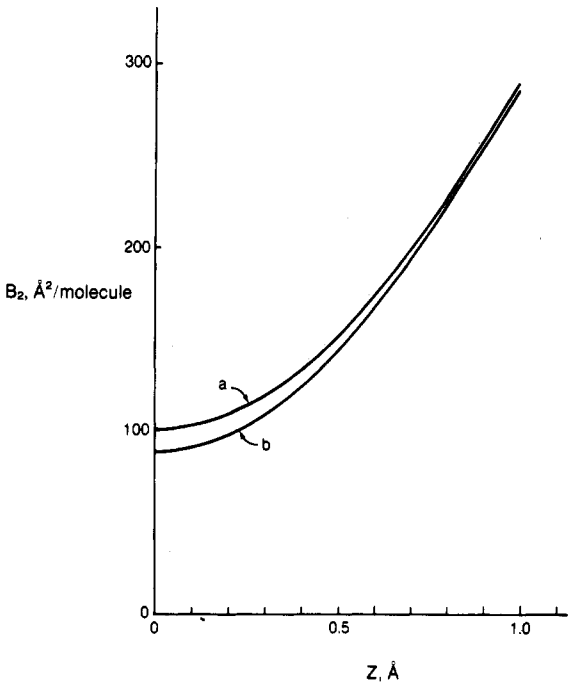

Figure 10. Comparison of results of B_2 for two models of PC head group with out-of-plane dipole moment ez (–e at interface, +e in oil): curve a for hard disk with central out-of-plane dipole only, eq 20; curve b for disk with asymmetric charge location and large in-plane dipole component, eq 21 (see Figure 9 and Table III).

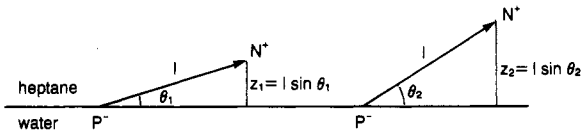

Figure 11. Coordinates for evaluation of B_2 for model of PC with fluctuating out-of-plane dipole moment with eq 24.

For the PC head group we define $U(z)$ in terms of the angle of tilt θ of the P^-N^+ vector into the heptane (see Figure 11). When l is the constant length of the P^-N^+ vector, and P^- is at the interface, $z = l \sin \theta$ may vary between $-l$ and $+l$. In terms of the angular coordinates θ_1 and θ_2 of two head groups, Hill's expression[24] defining the effective pair potential U_{12} for eq 20 becomes

$$e^{-U_{12}(r)/kT} - 1 = \left\{\int_{-\pi/2}^{\pi/2}\int_{-\pi/2}^{\pi/2}(e^{-U_1(\theta_1)/kT}e^{-U_2(\theta_2)/kT} - 1)(e^{-U_{12}(\theta_1,\theta_2,r)/kT} - 1)\cos\theta_1\cos\theta_2\,d\theta_1\,d\theta_2\right\} \Big/ \left\{\int_{-\pi/2}^{\pi/2}(e^{-U_1(\theta_1)/kT} - 1)\cos\theta_1\,d\theta_1\right\}^2 \quad (23)$$

The fluctuation part of the adsorption potential, $U(z)$, is of order kT. This potential for head group flopping is much smaller than the total adsorption potential of a lipid molecule at the interface. Therefore, since the potentials

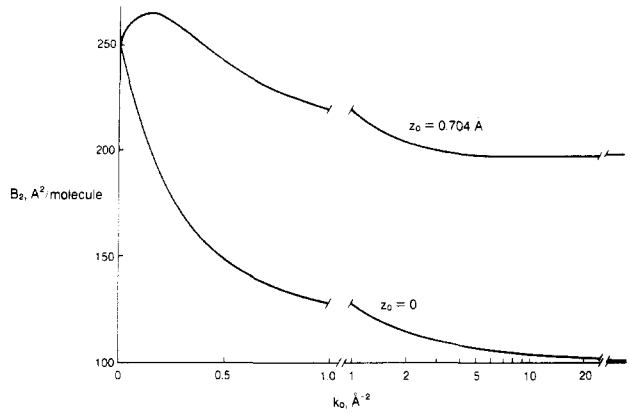

Figure 12. Results of B_2 evaluated with eq 20 and 24 for PC head group model of hard disk with out-of-plane dipole: P^- fixed at interface and N^+ fluctuating around z_0 in potential field with curvature (second derivative) k_0kT (eq 25).

U_1 and U_2 are negative and large, we may approximate eq 23 with

$$e^{-U_{12}(r)/kT} - 1 = \left\{\int_{-\pi/2}^{\pi/2}\int_{-\pi/2}^{\pi/2} e^{-U_1(\theta_1)/kT}e^{-U_2(\theta_2)/kT}(e^{-U_{12}(\theta_1,\theta_2,r)/kT} - 1)\cos\theta_1\cos\theta_2\,d\theta_1\,d\theta_2\right\} \Big/ \left\{\int_{-\pi/2}^{\pi/2} e^{-U_1(\theta_1)/kT}\cos\theta_1\,d\theta_1\right\}^2 \quad (24)$$

Equation 24 shows how the pair potential $U_{12}(\theta_1,\theta_2,r)$ is weighted by the Boltzmann factors of U_1 and U_2.

With eq 24 for the effective pair potential, $U_{12}(r)$, and eq 20 to evaluate B_2, we have used

$$\frac{U(\theta)}{kT} = \frac{k_0}{2}(l\sin\theta - z_0)^2 + \text{constant} \quad (25)$$

for the adsorption potentials $U(\theta_1)$ and $U(\theta_2)$ in eq 24, with l = 4.5 Å, z_0 = 0 and 0.7 Å, and various k_0 values. The factor k_0 represents a square law spring constant for head group flopping at the interface between $z = -l$ and $z = l$ around the position $z = z_0$ (see Figure 11). The results are shown in Figure 12 as a function of k_0. It is found that for large k_0, when the spring is stiff, the effect of fluctuations becomes insignificant. The values of B_2 for $k_0 = \infty$ are the same as those shown by the top curve in Figure 10 for $z = z_0$. Figure 12 shows that these asymptotic values are approached already within a few percent at k_0 = 5 Å^{-2}. For smaller k_0, that is, for shallower potential wells, the same limit is reached in both cases at $k_0 = 0$, for a random distribution of the angles θ_1 and θ_2. The slope of B_2 with k_0 is steeper for $z_0 = 0$ than for z_0 = 0.7 Å (see Figure 12). This is because stiffening the spring at $z_0 = 0$ more significantly reduces the important fluctuations (those deepest into the oil), whereas at z_0 = 0.7 Å, stiffening the spring from $k_0 = 0$ only serves to reduce the fluctuations into the water phase, which are unimportant for repulsion. The latter thus leads to the small increase in B_2 for stiffer spring constants near $k_0 = 0$.

9. Third Virial Coefficient for Hard Disks with Central, Perpendicular Dipole

So far we have concluded that a suitable model for the pair interaction between PC head groups is a hard disk, with radius a = 4 Å and a dipole component normal to the interface. We now investigate the consistency of this model with the triplet interactions measured by the third virial coefficient B_3.

We start with the general expression for B_3 in two dimensions, relating to three particles whose positions and orientations in a plane with area A are given by the three

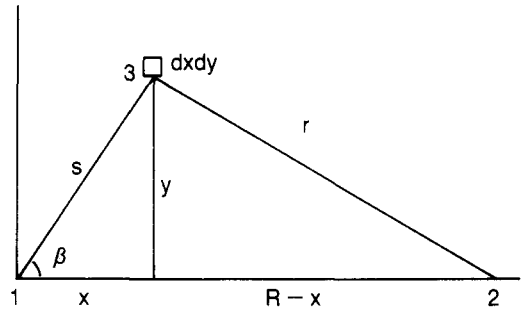

Figure 13. Bipolar coordinates in eq 27 and 28.

Table IV. Results for Hard Disks with Radius 4 Å and Central Dipole Charges −e at Interface and +e at Distance z into Heptane

z_r, Å	B_2, Å²/molecule	B_3, Å⁴/molecule	B_3/B_2^2
0	100.5	7.9×10^3	0.782
0.3	119.6	8.0×10^3	0.600
0.5	152.4	8.95×10^3	0.385
0.7	199.3	12.0×10^3	0.303
0.9	258.0	18.4×10^3	0.276

sets of coordinates r_1, r_2, and r_3. We assume the dipole interactions are pairwise additive. Then we have the potential $U(r_1,r_2,r_3) = U_{12} + U_{13} + U_{23}$ between the three particles, and the third virial coefficient is given by[24]

$$B_3 = -\frac{1}{3A}\int\int\int (e^{-U_{12}/kT} - 1)(e^{-U_{13}/kT} - 1)(e^{-U_{23}/kT} - 1)\,dr_1\,dr_2\,dr_3 \quad (26)$$

When the pair potentials do not depend on the orientation of the particles, eq 26 can be reduced with a transformation to bipolar coordinates, used by Hill[25,27] in the three-dimensional case of B_3. Let the interparticle distances be $R = r_{12}$, $s = r_{13}$, and $r = r_{23}$ (see Figure 13). Then the pair potentials are $U_{12} = U(R)$, $U_{13} = U(s)$, and $U_{23} = U(r)$. With particle 1 as origin, we have $\int dr_1 = A$, $\int dr_2 = 2\pi R dR$, and $\int dr_3 = dxdy$. With the relations $s^2 = x^2 + y^2$ and $r^2 = y^2 + (R - x)^2$, the Jacobian of the transformation of the coordinates (x,y) to (s,r) leads to

$$dr_3 = 2dxdy = \frac{2sr}{yR}dsdr = \frac{2rdsdr}{R\sin\beta} \quad (27)$$

The factor 2 is introduced because we allow only positive values of y. With $\cos\beta = (s^2 + R^2 - r^2)/2sR$ and the positive root $\sin\beta = [(1 + \cos\beta)(1 - \cos\beta)]^{1/2}$, dr_3 can now be expressed as a function of R, s, and r. With the same integration limits as in the three-dimensional case,[25] eq 26 becomes

$$B_3 = -\frac{8\pi}{3}\int_0^\infty R\,dR\int_0^\infty s\,ds\int_{|R-s|}^{R+s}[\{(1 - e^{-U(R)/kT}) \times (1 - e^{-U(s)/kT})(1 - e^{-U(r)/kT})r\,dr\}/\{((s + R + r)(s + R - r)(s - R + r)(-s + R + r))^{1/2}\}] \quad (28)$$

We have used eq 28 to evaluate B_3 for the earlier model of the PC head group, a hard disk with a 4-Å radius and central dipole charges −e at the interface and +e a distance z into the heptane (see previous section). Results of the numerical integrations for B_3 are given in Table IV for several values of z, along with the corresponding results for B_2 from eq 20, and of the ratio B_3/B_2^2. For $z = 0$ the well-known results[8] are $B_2 = 2\pi a^2$ and $B_3 = 0.782B_2^2$.

The theoretical results for B_3 shown in Table IV may be compared with the experimental values in Table II. For large repulsions, at 25 °C, the model reproduces the experimental values of B_2 and B_3 fairly well for $z \cong 0.8$ Å.

On the other hand, for small repulsions, at 5 °C, where B_2 corresponds to $z \cong 0.3$ Å, the calculated value of B_3 is far too small, by a factor of order 2.5. A possible explanation is in the contributions of dipole fluctuations. As shown above in Figure 12 and by results presented elsewhere,[28] such fluctuations may raise the calculated B_2 values significantly, in particular for small (average) dipoles, i.e., for small z. The same might be true for B_3, thus changing the quantitative relationship between B_2 and B_3. Actual calculations of B_3 for hard disks with fluctuating dipoles, corresponding to eq 20 and 24 for B_2, would require extensive computer time for six-dimensional integrations and were not attempted.

The work presented here is based on the virial method which, at least in our application, is an expansion at density $\Gamma = 0$; that is, B_2 and B_3 are taken at $\Gamma = 0$. Any extrapolation of results to finite monolayer densities or to bilayer membranes implies that the PN vector inclination is independent of the head group density and is the same as at $\Gamma = 0$. Any variation with Γ of this dipole orientation changes the pair interaction between head groups, and hence, changes B_2. Formally, such variations may be treated with a Taylor expansion

$$B_2(\Gamma) = B_2(\Gamma=0) + \left(\frac{dB_2}{d\Gamma}\right)_{\Gamma=0} \Gamma + \ldots \qquad (29)$$

and the amended virial expansion would be

$$\frac{\Pi}{kT} = \Gamma + B_2(\Gamma=0)\Gamma^2 + \left\{B_3(\Gamma=0) + \left(\frac{dB_2}{d\Gamma}\right)_{\Gamma=0}\right\}\Gamma^3 + \ldots \qquad (30)$$

We have shown that with a head group model without out-of-plane fluctuations the experimental B_2 values are well reproduced, while the calculated $B_3(\Gamma=0)$ results are at least of the same order as the coefficients of Γ^3 from experimental pressure–area isotherms and are thus reasonable. It would be of interest to study the consistency of B_2 and B_3 further for the head group model with out-of-plane fluctuations already used for B_2. A demonstrated insignificance of the term $dB_2/d\Gamma$ in eq 30 would lend much confidence to extrapolations of the present results for PC head group inclinations to more condensed structures.

10. Conclusions

We have determined the second and third virial coefficients, B_2 and B_3, and their temperature dependences from the data of Taylor et al.[2] of lateral pressure–area isotherms of phosphatidylcholines at the heptane/water interface. At low densities there is a large repulsion among the head groups, a repulsion that increases strongly with temperature. At low temperature (5 °C), the repulsion is well described by the hard-core interactions. The anisotropy due to the elongated shape of the head groups contributes little; the principal hard-core repulsion is suitably described by modeling the phosphatidylcholine head groups as hard disks of 4-Å radius. At higher temperatures, the dipole interactions also become important. The contribution of the dipole moment that lies in the bilayer plane is small and net attractive. We conclude that the most important dipole interaction is the out-of-plane component due to the displacement of the N^+ end of the P^-N^+ head group dipole into the oil phase by less than 1 Å. The very strong head group repulsions among phosphocholines is extremely sensitive to small changes in out-of-plane displacement. In addition, evidence regarding B_3 is strongly suggestive that this model is applicable to phospholipids at higher surface densities, as found in bilayer membranes.

The present paper does not address the issue of the balance of forces that cause the N^+ end of the dipole to be directed toward the oil phase. We present theory elsewhere for that purpose, of predicting head group orientation as a function of temperature and as a function of head group structure of the various phospholipids.[28]

Acknowledgment. This work has been supported by grants from the NIGMS and from the PEW Scholars Foundation to K.A.D. We thank Prof. Joe Bentz for helpful comments and critical reading of the manuscript.

Registry No. Heptane, 142-82-5; dioctadecylphosphatidylcholine, 4539-70-2; 1,2-dilauroylphosphatidylethanolamine, 42436-56-6.